A constant head well permeameter formula comparison: its significance in the estimation of field-saturated hydraulic conductivity in heterogeneous shallow soils

N. A. L. Archer, M. Bonell, A. M. MacDonald and N. Coles

ABSTRACT

We evaluate the application and investigate various formulae (and the associated parameter sensitivities) using the constant head well permeameter method to estimate field-saturated hydraulic conductivity (*Kfs*) in a previously glaciated temperate landscape in the Scottish Borders where shallow soils constrain the depth of augering. In finer-textured soils, the Glover equation provided *Kfs* estimates nearly twice those of the Richards equation. For this environment, we preferred the Glover equation with a correction factor for the effect of gravity, which does not include soil capillarity effects because: (1) the low depth to diameter ratio of the auger holes (AH) required in the shallow stratified soils of temperate glaciated environment needs a correction for gravity; (2) the persistently moist environment and the use of long pre-wetting times before measurements seem to reduce the effect of soil capillarity; (3) the Richards equation is dependent on accurate α^* values, but the measured AH intersected soil horizon boundaries that had different soil structure and texture, causing difficulty in selecting the most appropriate α^* value; (4) when comparing the different solutions to estimate *Kfs* using the constant-head well permeameter method against the AH method and ponded permeameter measurements, the Glover solution with a correction for gravity gave the best comparable result in fine-textured soil.

Key words | constant-head well permeameter, Guelph permeameter, hydraulic conductivity, infiltration, unsaturated soil

N. A. L. Archer (corresponding author)
A. M. MacDonald
British Geological Survey,
Murchison House, West Mains Road,
Edinburgh EH9 3LA, Scotland,
UK
E-mail: *nicarc@bgs.ac.uk*

N. A. L. Archer
Previously at: UNESCO Centre,
University of Dundee,
Perth Road, Dundee DD1 4HN,
Scotland,
UK

M. Bonell
UNESCO Centre,
University of Dundee, Perth Road,
Dundee DD1 4HN, Scotland,
UK

N. Coles
Centre for Ecohydrology,
University of Western Australia,
32 Stirling Highway, Crawley WA 6009,
Australia

INTRODUCTION

Reliable field estimates of field-saturated hydraulic conductivity (*Kfs*) (Bouwer 1966; Talsma 1987) in unsaturated soils are prerequisites for estimating water flow through soil profiles and are essential in estimating rates of soil water infiltration and soil permeability. Measurements of field-saturated hydraulic conductivity, for example, have been used to investigate land cover effects on the dominant stormflow pathways (Elsenbeer *et al.* 1999; Chappell *et al.* 2007; Bonell *et al.* 2010), water flow modelling and solute transport for drainage investigation (Noshadi *et al.* 2012), development of class pedotransfer functions (Lilly 2000) and estimating permeability of superficial deposits for characterising groundwater/surface water interactions (MacDonald *et al.* 2012).

The early development to more rapidly measure *Kfs* from a 'thin line source' (as defined by Talsma & Hallam 1980) using a constant-head well permeameter (CHWP) or simplified well permeameter was undertaken and described by Talsma & Hallam (1980). Through the use of the CHWP approach, *Kfs* could be more rapidly determined (Talsma & Hallam 1980; MacKenzie 2002) vis-à-vis its predecessor the 'shallow well pump-in method' (Boersma 1965; Bouwer & Jackson 1974). This instrument consists of an outer acrylic tube that contains the water for soil water infiltration and an inner smaller air entry tube. Vertical adjustable legs allow the tube to maintain a constant head height in an augered hole. The CHWP is particularly appropriate to deeply weathered soils where the water

doi: 10.2166/nh.2014.159

table occurs below the ground surface and the H/a ratio [H being the wetted auger hole (AH) depth, a being the AH radius] is preferably near to 10 (Talsma & Hallam 1980; Talsma 1987); see review in Mackenzie (2002). However, like its predecessor the 'shallow well pump-in method' (Talsma 1960; Bouwer & Jackson 1974), the CHWP was theoretically still based on the assumptions of the Glover solution (Zangar 1953), which corresponds to a line source from the bottom of the AH ($H = 0$) to the water surface ($h = H$) with no line sink (Reynolds *et al.* 1983). The Glover solution was re-examined by Reynolds *et al.* (1983), who then provided improved approximations (C values) of pressure gradients derived from various line sources with various source strength distributions.

The development of the Guelph permeameter (Reynolds & Elrick 1986) later provided analytical solutions of the Richards equation, which accounts for both the apparent effect of saturated and unsaturated components of flow from an AH (Elrick & Reynolds 1992). Using a Guelph permeameter requires the determination of a C factor and α^*. This C factor is a dimensionless shape factor approximating unsaturated steady-state flow out of an uncased, cylindrical hole into unsaturated soil and is derived from numerical simulations. Further, this factor is primarily a function of H/a ratio and has a secondary dependence on soil type (Elrick & Reynolds 1986). The α^* parameter is the ratio of *Kfs* to matric flux potential (ψ_m) and can be estimated using the two-ponded height technique, which uses two or more H depths. Alternatively, this ratio can be determined by the one-ponded height technique that *a priori* requires a soil description to determine the soil structure being measured which then leads to a predetermined α^* using a 'look-up' table (Elrick *et al.* 1989).

Using the two-ponded height technique to estimate α^* often produces negative *Kfs* values, as was experienced by Lilly (1994) in an earlier Scottish study. Negative *Kfs* values have been attributed to random soil heterogeneities and systematic soil textural changes with depth (Salverda & Dane 1993). The one-headed technique requires soil descriptions to describe soil texture/structure to determine which α^* value to use (Elrick *et al.* 1989). Elsewhere Bosch (1997) investigated the sensitivity of the Guelph permeameter solution to variations of α^* and found the greatest uncertainty in error occurred in the estimate of α^* when $\alpha^* < 0.015\ \text{mm}^{-1}$, which corresponds to fine-textured and compacted clays. Bosch (1997) also calculated that the misinterpretation of describing the soil structure to be medium to fine sand ($0.012\ \text{mm}^{-1}$), rather than unstructured fine-textured soil ($0.004\ \text{mm}^{-1}$), could result in *Kfs* being overestimated by 140%. A study by Laase (1989) compared the two-ponded height technique with the one-ponded height approach, and concluded that the one-ponded height technique was preferred, because it produced a smaller variance of *Kfs* results than the two-ponded height technique.

As described by Talsma (1987), overestimation of field saturated hydraulic conductivity (*Kfs*) can occur if capillarity of the soil surrounding the saturated region of an AH is disregarded, and this is particularly important for fine-textured soils that have low α^* values, or H/a ratios which fall below 5 (Reynolds *et al.* 1983). To counter such concerns, Talsma & Hallam (1980) recommended respectively a 10 or 20 min pre-wetting period for AHs inserted in 'wet' and 'dry' soils. On the other hand, in a comparative study of various field methods in gley-type soils, Chappell & Lancaster (2007) determined that of all the errors embedded within *Kfs* results, by far the most important was the smearing factor, that is, smearing of the cavity walls as a result of augering. From early work by Talsma (1960) in an environment with marked dry/wet seasons in Australia, Talsma compared the *Kfs* ('shallow well pump-in method') with saturated hydraulic conductivity (*Ksat)* (AH pumping test) using the same AHs. He determined the *Kfs*/*Ksat* ratio to be about 0.5. Later this 50% underestimation of *Ks* based on *Kfs*, as determined by the CHWP (Talsma & Hallam 1980, including the Reynolds *et al.* (1983) correction) was further supported using data from an experimental basin study (Talsma 1987). Based on the limited range of Australian soils considered by Talsma (1987), he thus suggested the need to multiply *Kfs* by a factor of 2. The study of Chappell & Lancaster (2007) however indicated an even greater underestimation of *Ks* in terms of orders of magnitude when concerning gley soils.

In addition to smearing, it is also common to observe lower *Kfs* values measured by the Guelph permeameter compared with other methods such as the AH method (Talsma 1960; Gallichand *et al.* 1990), undisturbed soil cores (Scotter *et al.* 1982; Paige & Hillel 1993; Mohanty *et al.* 1994), and velocity and disc permeameters (Mohanty *et al.* 1994). There are various reasons for these differences, such as the possibility of smaller volumes of soil being

sampled by the Guelph permeameter (Mohanty *et al.* 1994), smearing created by augering or boring and silting-up of the hole (Koppi & Geering 1986; Talsma 1987; Chappell & Ternan 1997; Chappell & Lancaster 2007), or the lack of continuity of pores (Scotter *et al.* 1982) and air entrapment within the vadose zone, the latter of which slows down infiltration rates (Wang *et al.* 1998).

The CHWP method is recognised as being well suited to measuring deeply weathered regoliths such as those commonly found in the tropics and old landscapes (e.g. Australia, India) that have not experienced Quaternary glaciation. Less attention has been given to the application of the CHWP method in shallow soils under different land covers associated with previously heavily glaciated landscapes. Topsoils under forest and grassland have variable depths of organic horizons where horizons merge into each other within a shallow depth, and also the presence of a dynamic biological component (such as roots, detritivores and organic matter) can create larger macropores. In areas subject to glaciation, retreating ice and meltwater deposit variable amounts of clay, silt, sand and gravel within relatively small areas, creating a landscape of poorly-sorted deposits of variable particle size. As a result, the soils are heterogeneous, including coarse gravels in a fine soil matrix, silts and organic soils, some of which overlay weathered bedrock. This nature of the soils causes difficulties in classifying them into the appropriate α^* value class, as described by Elrick *et al.* (1989). Further, the finer silty alluvial soils pose problems for possible smearing effects by augering holes. In heterogeneous soils, it is not always possible to auger below 0.15 m, because of stony layers below this depth resulting in H/a ratios below 5. These circumstances cause problems in the determination of reliable *Kfs* measurements from the two-head height approach to determine α^* for different soil types.

There is therefore a requirement to investigate the most appropriate mathematical formulae for interpreting CHWP data in the heterogeneous soils common in previously glaciated areas. In this study, we explore the use of the CHWP method of Talsma & Hallam (1980) and we investigate more than one formula (and the associated various parameter sensitivities) to decide which mathematical solution is best to adopt for shallow glaciated soils. Our purpose for measuring *Kfs* is part of a study connected with Natural Flood Management (Werritty *et al.* 2010). A comparison of the upper soil permeability with extreme rainfalls using rainfall intensity duration frequency (IDF) was carried out and is described in Archer *et al.* (2013). Such an investigation required accurate and reliable *Kfs* measurements near the soil surface that are representative of field conditions. This created the basis for this paper. Thus, in this study we aim to understand how the different formulae affect the resulting *Kfs* values by carrying out a comparative analysis of results of different formulae applied to *in-situ* field data. We also make some preliminary measurements of *Ks* using the AH method (Van Beers 1985) to investigate the possible effect of AH smearing supplemented by surface measures of *Kfs* (Perroux & White 1988) on a flat floodplain zone.

Field site

The field site is in the Scottish Borders (55°42.9′N, 3°13′W) within the Tweed catchment and is located near Eddleston village in the Eddleston Water Catchment (Figure 1). It consists of a hillslope extending to a floodplain that varies from 0 to 22% gradient and has an altitudinal range from 192 to 255 m (above Ordnance Datum).

The field site area (Figure 2) is mainly agriculturally improved grassland, where cattle and/or sheep graze from spring to autumn. In the lowest-lying depression of the floodplain, a rush community (*Juncus effuses* with some *Ranunculus repens*) dominates the gley soils. Neighbouring the steep grazed slope is a *Pinus sylvestris* plantation, which was planted over 45 years ago. Further upslope, west of the river, the grazed grassland area borders onto Barony Castle, set in grounds of 10 ha, which contain old remnants of woodland dating back to 1536. Some of this woodland has been disturbed and partially cut down in the last 180 years and other areas have remained wooded for at least 500 years. Woodland species are mainly deciduous comprising of *Fagus sylvatica*, *Prunus spinosa*, *Quercus petraea*, *Betula pendula*, *Acer pseudoplatanus* and a few *Fraxinus excelsior*. Some *Pinus sylvestris* are also found in the woodland. Figure 2 shows the location of measurement points that are divided into four pairs, that is, each pair containing woodland and an adjacent grassland. Table 1 describes in detail these sites in terms of soil structure, superficial geology and land cover.

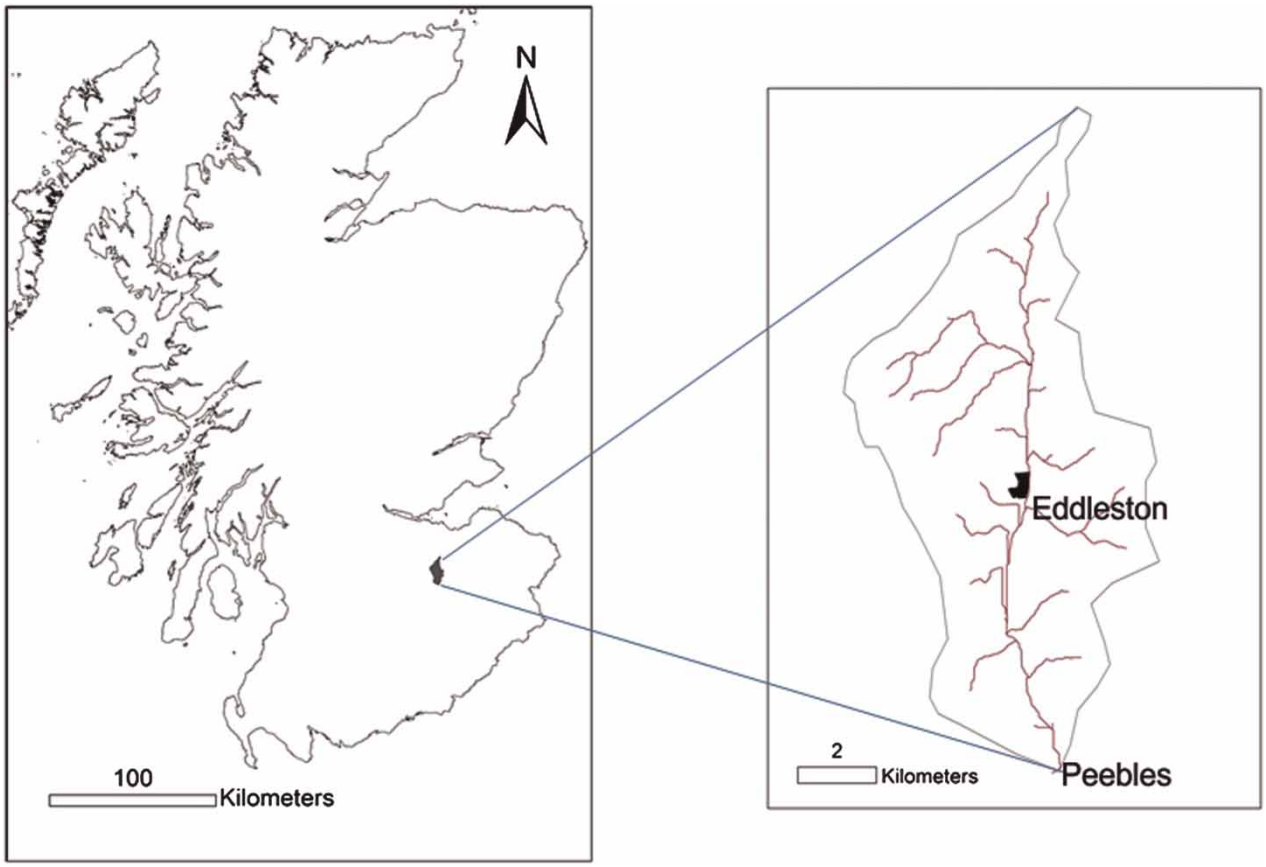

Figure 1 | The location of the field area in Scotland and in the catchment of the Eddleston Water.

According to a recent survey of the geology (British Geological Survey 2011), there is brittle very resistant rock (Ordovician meta-sandstone greywacke), which crops out near the soil surface on parts of the hillslope. Till outcrops are located between DW2 and G2. Most measured areas are located on Head deposits, which are typically gravelly sediments, derived from local materials transported by colluvial processes, and produce poorly-sorted, stony soils. DW1 and G1 have high contents of sand, which are likely to have been brought in by glacial meltwater from the north-west. Within the floodplain (FW4 and G4) mainly silts occur which formed as overbank deposits. Also there are some beds of coarse gravel and sand within this floodplain that were laid down by laterally migrating river channels. Soil texture, measured from soil samples taken from AHs, ranged from silt in the floodplain, fine to coarse gravels on the steeper slope, and subsequently sandy silt with some gravels on the upper flatter slopes. Clay content was relatively low throughout the site, being approximately 6% on the slope and up to 15% in the floodplain. The site is dominated by two Associations: Alluvium soils in the floodplain and Yarrow soils on the hillslope (Scotland Soil Survey Staff 1975), as shown in Figure 2. The Yarrow Association on the hillslope comprises brown earths developed on gravels derived mainly from greywackes, and can be classified as Cambisols in the World Reference Bank (WRB) soil classification system (WRB 2006). The topsoil is mainly strong brown to yellow-brown stony loamy sand, and the subsoils are coarse gravel. These soils drain easily and are associated with a low water-holding capacity (Bown & Shipley 1982). The Alluvium soils are relatively young alluvial sediments developed on freshwater alluvial deposits (Fluvisols in the WRB classification), mainly consisting of silts varying with some sand and clays. Fine to coarse gravels occur throughout the soil profile. The Alluvium soils are

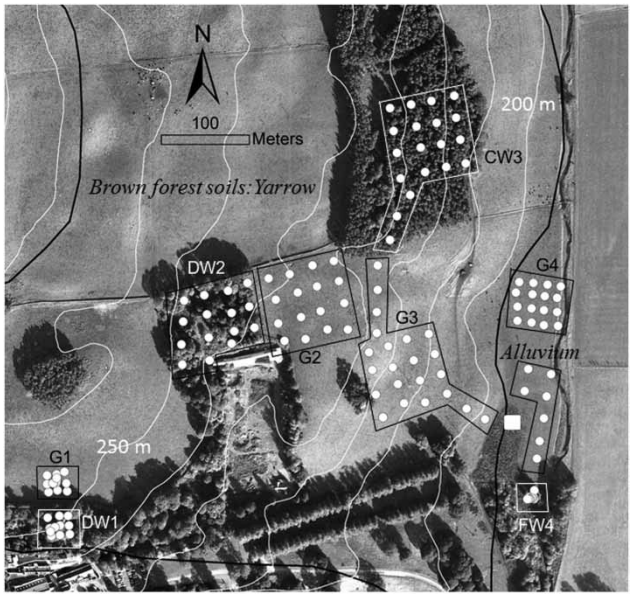

Figure 2 | Aerial photo of site area showing the locations of the CHWP measurements (white circles) and area of AH measurements (white square). Four AH measurements were carried out within the white square. PD measurements (Perroux & White 1988) were undertaken within G4 only. CHWP measurements were taken at two depths (0.04 to 0.15 m and 0.15 to 0.25 m) for DW1, G1 and G4. All other areas were measured at one layer (0.04 to 0.15 m). White lines represent contours and the black lines are the delineations of Associations shown in the Peebles soil map: Soil Survey of Scotland, systematic soil survey; sheet 24 & part of sheet 32. Scale 1:250,000 (Soil Survey of Scotland Staff 1975). © UKP/Getmapping Licence No. UKP2006/01.

poorly-draining depending on the occurrence of clay material and the presence of the water table in the floodplain.

METHODOLOGY

Description of soil structure

As the focus of this study was to measure *Kfs* in the upper soil surface, the depths at which soil horizons changed within the shallow topsoil were noted. Some soil horizons (particularly organic horizons) changed to other horizons within 0.1 m. To provide an understanding of such soil structure, soil descriptions were taken for each augered layer, that is, 0 to 0.15 m and 0.15 to 0.25 m.

Soil texture was determined by taking bulk samples from four AHs in each measured area for particle-size analysis. This was undertaken by dry sieving the bulk soil samples into sieve sizes: 60, 20, 6.3 and 2 mm and the particle size distribution of material <2 mm was measured using a Beckman and Coulter LS13 320 Laser Diffraction Particle Size Analyser.

Field experimental methods

Figure 2 shows the distribution of points where *Kfs* was measured. Three measurement techniques were available for use in the field: the constant-head well permeameter (CHWP) (Talsma & Hallam 1980), the ponded disc permeameter (PD) developed by Perroux & White (1988) and the AH method (Van Beers 1985). Each of these methods is well described in the literature. The application of each method for each point, where valid, was determined by field conditions as described in the following sections.

CHWP method

The CHWP was the only method used to measure *Kfs* in all sites, because it is able to measure *Kfs* in areas that have steep topography and in topsoils which are above the water table. A preliminary survey of the hillslope found a gravel layer prevented augering below 0.15 m in the steepest part of the hillslope. So that all areas of the hillslope and floodplain could be compared, all AHs were augered to 0.15 m. To avoid interference from the soil surface, the CHWP was set to measure 0.04 m below ground surface. In the 500 year-old deciduous woodland, adjacent grassland and the floodplain, it was possible to auger another hole to 0.25 m because the gravel layer was deeper in these areas. Therefore, *Kfs* was measured at a soil depth between 0.15 and 0.25 m in these three areas (shown in Figure 2). Before pre-wetting the AH for 20 min, pea gravel was added into the hole to prevent the cavity walls from collapsing. For very permeable soils the AHs were pre-wetted for a longer time, to ensure the fall of water reached a steady state.

The AH method

The AH method measures *Ks* below the water table and is considered to measure actual *Ks*, because measurements are taken below groundwater level, where soils are completely saturated. The only area where the water table was near the surface was in a small, marshy grassland area on the floodplain. For this reason, the AH method could be used only in

Table 1 | Summary of soils measured for each site area, describing soil horizons, texture, structure and superficial geology

Site area	Description	Topsoil description	Soil structure and texture	Superficial geology
G1	Improved grassland >265 years	0 to 0.04 m grass root mat. A horizon extends from 0.05 to 0.25 m and grades into a B Horizon. Gravels exist throughout, but coarse gravel increases in the B horizon below 0.25 m depth.	Loamy sand. Granular, crumb structure 0 to 0.04 m, becomes sub angular blocky around 0.2 m.	Glaciofluvial gravel and sand.
DW1	Deciduous woodland, mature beech >500 years	0 to 0.10 m litter layer. Humus layer up to 0.05 m. Organic layer extends to 0.15 grading into A horizon between 0.15 m to 0.30 m. Gravel B horizon extends into A horizon around 0.25 m. Organic horizons variable depending on distance from trees. Gravels increase around 0.25 m depth.	Loamy sand. Granular, crumb, structure to depths over 0.2 m, below this depth can become blocky or structureless, depending on sand content and presence of roots.	Glaciofluvial gravel and sand.
G2	Improved grassland >265 years	Dense grass root mat 0 to 0.05 m. A horizon to 0.20 m. Coarse gravel throughout profile, at variable depth increasing from 0.20 m.	Sandy loam. Granular, crumb structure 0 to 0.4 m, becomes sub angular blocky around 0.2 m.	Till occurring within the upper half of the site area. The rest of the area underlain by Head.
DW2	Deciduous mixed woodland <160 years	0 to 0.05 m litter layer. Humus layer variable thickness from 0.01 to 0.05 m. Organic layer between 0.10 m to below 0.20 m depth, extending into A horizon. Organic horizons variable depending on distance from trees. Gravels exist throughout, but increase around 0.20 m.	Sandy loam. Granular, crumb, structure to depths over 0.15 m, below this depth can become blocky or structureless, depending on sand content and presence of roots.	Till occurring within the lower half of the site area. The rest of the area is underlain by Head.
G3	Improved grassland >265 years	Dense grass root mat 0 to 0.05 m. Silty A horizon extends to around 0.20 m. Coarse gravel throughout profile, increasing at 0.20 m.	Sandy loam. Granular, structure 0 to 0.05 m becomes sub angular blocky around 0.1 m.	Gravels derived from bedrock.
CW3	Conifer plantation 50 years	0 to 0.05 m litter layer. Dark humus layer variable thickness from 0.01 to 0.05 m. Organic silt A horizon extends from 0.10 m to below 0.15 m and colour changes to red-brown, showing possible illuviation of organic colloids. Cobbles present from 0.15 m grading into a B horizon and in some points reaching a shallow C horizon.	Sandy loam. Granular, crumb structure 1 to 0.15 m. Becomes blocky below 0.15 m.	Gravels derived from bedrock.
G4	Improved grassland >265 years	0 to 0.04 m organic layer. Clay silt A horizon extends between 0.04 m to below 0.3 m. Gravel occasionally present from 0.2 m. Some gleying below 0.2 m.	Loam. Granular, crumb structure 0 to 0.04 m. Becomes unstructured around 0.1 m.	Recent riverine alluvial deposits.
FW4	Deciduous woodland, mature willows < 180 years	0 to 0.08 m, highly heterogeneous organic layer. A horizon extends from 0.08 m to below 0.3 m. Areas of gleying occur around 0.015 m soil depth.	Loam. Granular structure 0 to 0.1 m, becomes unstructured 0.1 to 0.15 m.	Recent riverine alluvial deposits.

The mix of letters indicates G is grassland cover, W relates to woodland cover, D is deciduous woodland, C is conifer and F is floodplain.

a very small area (Figure 2), where holes were augered from 0.5 to 1 m depths. The water in the AH was rapidly pumped out and then left to be replaced by groundwater. This procedure was done several times to open the soil pores and reduce the effect of smearing. The rate of recovery was measured by the rate of rise of the water table within the AH.

The PD method

This method measures *Kfs* at the ground surface and can be undertaken only on flat ground where the water table is at least 0.5 m below ground; the only area to fit these criteria was on the floodplain in area G4 (Figure 2). Therefore in the G4 area, PD and CHWP measurements were taken at adjacent locations within 0.5 m of one another.

Soil conditions during measurements

Field measurements took place during two summers (2011, 2012), when weather conditions were dry. Initial soil water contents were measured gravimetrically from cores taken at the same time as *Kfs* measurements and capacitance probes (*ThetaProbes*: ML2x Delta-T, Cambridge, UK) automatically logged soil water content in the grassland. Soil water content ranged from 15% to 35%. Such water contents are below field capacity in all soil types, ensuring that there was no free water available to flow into the AHs from surrounding soil horizons.

Effect of smearing

In an attempt to avoid smearing, a hard nylon cylindrical brush was used to lightly scrape the sides of each augered hole. This was done mainly in the floodplain, where silt contents were higher, but in AHs that contained more sand and gravel, this was not done.

Because silty gley soils were mainly found in the floodplain and the effects of smearing for such soils have been found to introduce errors (Chappell & Lancaster 2007), we investigated the CHWP results for the floodplain in more detail. Shallow soil descriptions taken in the areas where the AH method was used (Figure 2) were found to be similar to the grassland floodplain area (G4, Figure 2). Because of soil similarity between the wetland and drier grassland floodplain it was considered that measurements using the AH method could be compared to the CHWP data from the floodplain area. However, the scope for a direct comparison between *Kfs* and *Ks* within the floodplain zone was limited, as there was only a small area in the wetland where the soils below the water table are comparable to soils above the water table in the floodplain zone. Therefore in this small area, only four AHs could be augered to depths between 0.47 and 0.77 m.

As there was limited data from the AH method, we also compared the CHWP measurements in the floodplain zone with the results from the PD method, as it could be used as a 'benchmark' to compare *Kfs* values measured at soil depths between 0.04 and 0.15 m. Such steps were taken because the PD method measures surface *Kfs* and does not require the augering of a hole; therefore no smearing effects occur. In making such comparisons it is acknowledged that the surface soil conditions would have relatively higher *Kfs* values because of the presence of an organic layer in the top 0.04 m of soil surface compared with the soil between 0.04 and 0.15 m depth, as measured by the CHWP. On the other hand, the *Kfs* estimates measured by the PD method are biased to the vertical component of *Kfs*, vis-à-vis the horizontal component for *Kfs* (CHWP) and *Ks* (AH method), so they are strictly not comparable. Nonetheless some inferences may still be possible linked to the effect of smearing.

Investigated formulae

For each formula investigated, the same field data from measured points (shown in Figure 2) were used; this included: steady-state flow out of an AH (Q), AH radius (a) and AH head height (H). The compared data all had H/a ratios of approximately 3. *Kfs* was calculated under five categories: (1) the Glover solution (Zangar 1953) based on the Laplace equation; (2) improvements of the Glover solution, where gravity is an added component (Reynolds *et al.* 1983) and the pressure head distribution along the AH wall is numerically solved; (3) adding the component of capillarity based on the Richards equation (Elrick *et al.* 1989); (4) taking away the component of capillarity using the Elrick *et al.* (1989) solution and calculating *Kfs* assuming only saturated flow; and finally (5) the effect of smearing (Talsma 1960; Talsma 1987) on the resulting values is investigated. Table 2 provides a key overview of the 10

Table 2 | Summary of the various solutions used in the sensitivity analysis

Solution ID	Reference	*Kfs* Eq. and *C* factor formulae	Assumptions	Percentage difference to Equation (1)
1	Glover solution (Equations (3) and (4)), p. 320 Elrick & Reynolds (1992)	[a] $Kfs = CQ/(2\pi H^2)$ $C = \sinh^{-1}\left(\frac{H}{a}\right) - \left(\frac{a^2}{H^2}+1\right)^{1/2} + 2/H$	Saturated flow, capillarity is zero and flow as a component of gravity is negligible, based on the Laplace solution.	
2A	Glover solution (Equation (2)) *C* factor calculated from Equation (3) (Reynolds *et al.* 1983)	$K_{fs} = CQ/2\pi H^2\left[1 + C/2\left(\frac{a}{H}\right)^2\right]$ $C = \sinh^{-1}(H/a) - \sqrt{(H/r)^2+1} + a/H$	Saturated flow, capillarity is zero and component of gravity added based on the Laplace solution.	+24%
2B	Glover solution. *C* factor calculated from the numerical solution (Reynolds *et al.* 1983)	The numerical factor *C* for $H/a = 3$ in saturated conditions was estimated from Fig. 1 p. 321 (Elrick & Reynolds 1992)	Saturated flow, capillarity is zero and component of gravity added based on the Laplace solution where gradient solution is obtained by solving numerically for steady-state head distribution.	+172%
3A	$\alpha^* = 0.36\ \text{cm}^{-1}$ (Elrick *et al.* 1989, Equation (13), p. 186), *C* factor Equation (1), p. 220, Zhang *et al.* (1998)	$Kfs = CQ/(2\pi H^2 + \pi a^2 C + 2\pi H/a^*)$ When $\alpha^* = 0.36\,\text{cm}^{-1}$ $C = \left(\frac{H/a}{2.074 + 0.093(H/a)}\right)^{0.754}$	Includes saturated and unsaturated flow. *C* value based on Richards Eq. includes components of gravity and capillarity.	+9%
3B	$\alpha^* = 0.12\ \text{cm}^{-1}$ (Elrick *et al.* 1989, Equation (13), p. 186), *C* factor Equation (1), p. 220, Zhang *et al.* (1998)	$Kfs = CQ/(2\pi H^2 + \pi a^2 C + 2\pi H/a^*)$ When $\alpha^* = 0.12\,\text{cm}^{-1}$ $C = \left(\frac{H/a}{2.074 + 0.093(H/a)}\right)^{0.754}$	Includes saturated and unsaturated flow. *C* value based on Richards Eq. includes components of gravity and capillarity.	−21%
3C	$\alpha^* = 0.04\ \text{cm}^{-1}$ (Elrick *et al.* 1989, Equation (13), p. 186), *C* factor Equation (2), p. 220, Zhang *et al.* (1998)	$Kfs = CQ/(2\pi H^2 + \pi a^2 C + 2\pi H/a^*)$ When $\alpha^* = 0.04\,\text{cm}^{-1}$ $C = \left(\frac{H/a}{1.992 + 0.091(H/a)}\right)^{0.683}$	Includes saturated and unsaturated flow. *C* value based on Richards Eq. includes components of gravity and capillarity.	−57%
3D	$\alpha^* = 0.01\ \text{cm}^{-1}$ (Elrick *et al.* 1989, Equation (13), p. 186), *C* factor Equation (3), p. 220, Zhang *et al.* (1998)	$Kfs = CQ/(2\pi H^2 + \pi a^2 C + 2\pi H/a^*)$ When $\alpha^* = 0.01\,\text{cm}^{-1}$ $C = \left(\frac{H/a}{2.102 + 0.118(H/a)}\right)^{0.655}$	Includes saturated and unsaturated flow. *C* value based on Richards Eq. includes components of gravity and capillarity.	−86%
4A	$\alpha^* = \infty$, $C \geq 0.12\ \text{cm}^{-1}$ (Elrick *et al.* 1989, Equation (13), p. 186), *C* factor Equation (1), p. 220, Zhang *et al.* (1998)	$Kfs = CQ/(2\pi H^2 + \pi a^2 C)$ When $C > 0.12\,\text{cm}^{-1}$ $C = \left(\frac{H/a}{2.074 + 0.093(H/a)}\right)^{0.754}$	Includes saturated flow with capillary flow removed. *C* value based on Richards Eq. includes components of gravity.	+35%

(*continued*)

Table 2 | continued

Solution ID	Reference	*Kfs* Eq. and *C* factor formulae	Assumptions	Percentage difference to Equation (1)
4B	$\alpha^* = \infty$, $C = 0.04\ \mathrm{cm}^{-1}$ (Elrick *et al.* 1989, Equation (13), p. 186), *C* factor Equation (2), p. 220, Zhang *et al.* (1998)	$Kfs = CQ/(2\pi H^2 + \pi a^2 C)$ When $C = 0.04\ \mathrm{cm}^{-1}$ $C = \left(\frac{H/a}{1.992 + 0.091(H/a)}\right)^{0.683}$	Includes saturated flow no capillary flow. *C* value based on Richards Eq. includes components of gravity.	+36%
4C	$\alpha^* = \infty$, $C = 0.01\ \mathrm{cm}^{-1}$ (Elrick *et al.* 1989, Equation (13), p. 186), *C* factor Equation (3), p. 220, Zhang *et al.* (1998)	$Kfs = CQ/(2\pi H^2 + \pi a^2 C)$ When $C = 0.01\ \mathrm{cm}^{-1}$ $C = \left(\frac{H/a}{2.102 + 0.118(H/a)}\right)^{0.655}$	Includes saturated flow no capillary flow. *C* value based on Richards Eq. includes components of gravity.	+29%

[a]The Glover solution is normally written: $K_{fs} = Q\left(\sinh^{-1}(H/r) - 1\right)/2\pi H^2$.

variations of the solutions used to calculate *Kfs* and these are described in detail below.

Solution 1

The Glover solution (Zangar 1953) is defined by:

$$Kfs = \frac{Q\left[\sinh^{-1}\left(\frac{H}{a} - 1\right)\right]}{2H^2} \quad (1)$$

where Q is steady-state flow out of the AH, H is AH head height and a is AH head height.

Solution 2A

Analysis of the Glover solution theory by Reynolds *et al.* (1983) demonstrated that the influence of gravity to steady-state flow is inversely proportional to the square of H/a ratio. This relationship, shown by Elrick & Reynolds (1992), is of particular importance when the ratio H/a is low, as the effect of gravity on the total flow out of the well hole is >30% when $H/a = 0.5$, but falls to only 1.5% when $H/a = 10$. To provide better approximations to the boundary conditions along the submerged wetted surface of the well, Reynolds *et al.* (1983) published improvements on the theory using Equation (2), defined by:

$$Kfs = \frac{CQ_t}{2\pi H^2\left[1 + \frac{c}{2}\left(\frac{a}{H}\right)^2\right]} \quad (2)$$

Based on the theory given by Reynolds *et al.* (1983), the shape coefficient, C for the Glover solution was calculated using:

$$C = \sinh^{-1}\left(\frac{H}{r}\right) - \sqrt{\left(\frac{r}{H}\right)^2 + 1} + \frac{r}{H} \quad (3)$$

Solution 2B

The influence of numerical *C* factor was also investigated, where the steady-state pressure head distribution in a cylindrical flow area surrounding the well is solved numerically. This procedure, as explained by Reynolds *et al.* (1983) p. 258, 'has the advantage of matching the pressure head distribution along the wall and base of the well exactly'.

Solutions 3A, 3B, 3C and 3D

As the Glover solution attributes all flow out of the cavity as saturated flow, unsaturated flow (or capillary flow) is

neglected. To include unsaturated flow, Elrick *et al.* (1989) developed the following solution:

$$Kfs = \frac{CQ}{\left(2\pi H^2 + \pi a^2 C + \frac{2\pi H}{\alpha^*}\right)} \quad (4)$$

The three terms in the denominator represent the approximate contributions of hydrostatic pressure, gravity and capillarity respectively. α^* is given by

$$\alpha^* = \frac{Kfs}{\varphi_m} \quad (5)$$

where φ_m is the matric flux potential. α^* can be calculated in the field by ponding water at two different heights in the same well and then solving the simultaneous equations for *Kfs* and φ_m (Elrick *et al.* 1989), or by taking a soil description for each well to classify the soil into four textural groups described by Elrick *et al.* (1989), which then relates to four pre-defined α^* values: 0.01 cm^{-1} for compacted structureless, clayey or silt materials, 0.04 cm^{-1} for fine textured and unstructured soils, 0.12 cm^{-1} for structured soils from clays through loams, and 0.36 cm^{-1} for coarse gravelly sands, which can include highly structured soils with cracks and macropores (Elrick *et al.* 1989). Each soil type has a different *C*, which is dependent on the H/a ratio (Reynolds & Elrick 1987). For each of the four soil textural groups, the *C* values are based on the Richards equation and were calculated from empirical functions developed by Zhang *et al.* (1998).

Solutions 4A, 4B and 4C

To assume zero capillarity, α^* was set to infinity by setting the term $2\pi H/C$ in Equation (4) to zero and the *C* factor was set to the three soil types.

Soil structure and the choice of α^* to calculate *Kfs* using Equation (4)

Investigations which use Equation (4) should take care to auger into homogenous soil horizons, as described by Lilly (1994). The latter excavated a soil pit to identify the horizon depths so that the wetted length, *H* (e.g. Equation (1)) did not cross a soil horizon boundary. In this study, such steps could not be undertaken, because of the shallow nature of the soils, especially on the steeper slopes, and the organic soil horizons often merge into A horizons within shallow soil depths. This results in some AHs intersecting more than one horizon within some of the sites and thus the wetted length *H* invariably crosses these horizons. In such circumstances, the inclusion of more than one α^* value (as provided by Elrick *et al.* (1989)) could be used within the same AH. To investigate this problem, possible α^* values (as described in section 'Solutions, 3A, 3B, 3C and 3D') were used where AHs for different sites and soil layers crossed more than one horizon. The results from using Equation (4) with different α^* are compared with the results from using the Laplace solutions (i.e. solutions 1 and 2A), to decide the best analytical solution for measuring soils where the wetted length *H* crosses more than one soil horizon.

RESULTS

Description of topsoil structure and texture

Table 1 summarises the AH soil descriptions for each site area. The depth of the organic horizon was particularly variable under the woodland areas, and because organic horizons changed to A/B horizons within the shallow layer of the topsoil, many AHs intersected these boundaries.

Field data used in the comparative analysis of different formulae

The high diversity of soil structure and texture that also changes within shallow depths (as described in Table 1) provides a large range of steady-state flows out of the AH (*Q*), ranging from 1 $mm^3\,s^{-1}$ (in the floodplain zone) to 9,505 $mm^3\,s^{-1}$ (in the old deciduous forest), as shown in Table 3. The areas of highest variability occurred in the woodland areas (Table 3).

Comparative analysis of CHWP formulae to calculate *Kfs*

Figure 3 illustrates the calculated *Kfs* for each of the described solutions against the Glover solution (Equation (1)).

Table 3 | Site IDs relate to Figure 1. *H* is the head height of water in the AH, *a* is the radius of the AH, *Q* is the steady-state rate of water entry into the AH, Max. *Q* is the maximum steady-state infiltration and Min. *Q* is minimum steady-state infiltration

Site ID	Number of measurements	Soil depth (m)	Mean *H* (mm)	Mean *a* (mm)	[a]Mean *Q* ($mm^3\ s^{-1}$)	SE	Max. *Q* ($mm^3\ s^{-1}$)	Min. *Q* ($mm^3\ s^{-1}$)
DW1	13	0.04–0.15	110	36	2,686	764	9,505	166
DW1	13	0.15–0.25	100	34	498	87	1,175	166
G1	13	0.04–0.15	110	33	407	182	2,143	60
G1	13	0.15–0.25	100	33	194	33	503	83
DW2	16	0.04–0.15	110	34	2,305	536	8,045	617
G2	16	0.04–0.15	110	34	420	69	1,382	202
CW3	16	0.04–0.15	110	37	889	184	2,886	313
G3	16	0.04–0.15	110	36	653	538	2,239	152
FW4	12	0.04–0.15	110	33	154	516	4,812	1
G4	16	0.04–0.15	110	32	28	13	216	7
G4	16	0.15–0.25	100	33	48	12	199	16

[a]Mean *Q* is the geometric mean because the *Kfs* is log normally distributed.

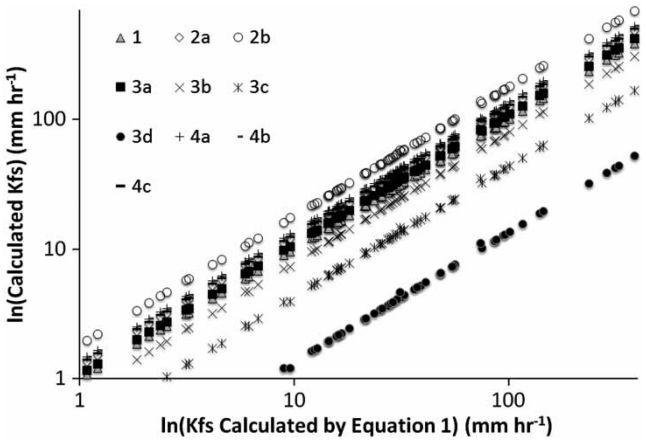

Figure 3 | Comparison of logarithmic *Kfs* values calculated using different formulae described in Table 2 against the Glover solution (Equation (1)), shown as 1:1 line. The number of data points was reduced to provide more clarity to the graphs.

In addition, Table 2 summarises the various solutions and assumptions used in the comparative analysis and the magnitude of difference between each solution against the Glover solution (Equation (1)).

Figure 3 illustrates that the *Kfs* values calculated from the Glover solution (Equation (1), shown as solution 1) are located midway between the Reynolds *et al.* (1983) solution 2B, which obtained 172% higher *Kfs* values than the Glover solution (Table 2) and the Elrick *et al.* (1989) solutions 3A, 3B, 3C and 3D where the addition of capillary flow for the different soil types gives lower *Kfs* values. The lower the α^* value, the lower the estimation of *Kfs* as is shown in Table 2. For example when $\alpha^* = 0.01\ cm^{-1}$, calculated *Kfs* values are 86% lower than *Kfs* values calculated by the Glover solution, whereas $\alpha^* \geq 0.12\ cm^{-1}$ produces *Kfs* values only 21% lower than the Glover solution. Removing the effect of capillarity from the Richards equation increases the *Kfs* values up to 36% higher than the *Kfs* values calculated by the Glover solution (Table 2). The net result is that the *Kfs* values are similar to solution 2A, where the addition of the gravity flow component provides 24% higher *Kfs* values than the Glover solution (Table 2). The three shape curve factors (*C*) cause little difference to *Kfs* values, when the *H*/*a* ratio is near 3 (as is the case in this study). This is because the shape factor curves are very similar at low *H*/*a* ratios, as shown by Zhang *et al.* (1998).

Effects of soil structure and α^* values for Equation (4)

Table 4 compares the geometric means of calculated *Kfs* values using the Richards equation (3A, 3B and 3C, Table 2) and two Glover solutions (1 and 2A, Table 2) for the different measured sites (shown in Figure 1) and soil depths. These particular solutions were chosen because they are the most common formulae used in field research to calculate *Kfs*. To calculate the Richards equation, the most appropriate α^* value for each site and soil depth was chosen on the basis of soil descriptions shown in Table 1.

Table 4 | Comparison of geometric mean *Kfs* calculated from Solution 1 (the Glover solution), Solution 2A (the Glover solution corrected for gravity) and Solutions 3A, 3B and 3C (the Richards equation, using one of the α^* values: 0.04, 0.12 and 0.36 cm^{-1}) for each site and measured soil layers. 0.01 cm^{-1} α^* is not included, because it was considered that none of the soils fitted into this category. The values in brackets are selected α^* values used in the calculation. More than one α^* is added to some sites, when it was difficult to define which α^* to use where the AH intersected more than one soil horizon

Site ID	Soil depth (m)	Mean *Kfs* (3A, 3B, 3C) (mm hr^{-1})	Mean *Kfs* (1) (mm hr^{-1})	Mean *Kfs* (2A) (mm hr^{-1})
DW1	0.04–0.15	(0.36 cm^{-1}) 120	102	130
DW1	0.15–0.25	(0.36 cm^{-1}) 23, (0.12 cm^{-1}) 16	21	26
G1	0.04–0.15	(0.36 cm^{-1}) 18, (0.12 cm^{-1}) 13	18	21
G1	0.15–0.25	(0.12 cm^{-1}) 7, (0.04 cm^{-1}) 4	8	10
DW2	0.04–0.15	(0.36 cm^{-1}) 106	98	120
G2	0.04–0.15	(0.12 cm^{-1}) 14, (0.04 cm^{-1}) 8	18	21
CW3	0.04–0.15	(0.36 cm^{-1}) 38	34	42
G3	0.04–0.15	(0.12 cm^{-1}) 21, (0.36 cm^{-1}) 29	26	32
FW4	0.04–0.15	(0.36 cm^{-1}) 5, (0.12 cm^{-1}) 5	6	7
G4	0.04–0.15	(0.12 cm^{-1}) 1, (0.04 cm^{-1}) 0.64	2	2
G4	0.15–0.25	(0.04 cm^{-1}) 1	2	3

Sometimes two α^* values are given when the AH crosses two different horizons. For example, using soil descriptions for depth 0.04 to 0.15 m for site G2 (Figure 4(ii)), the upper half of the AH was considered to be more permeable than the lower part because of the soil structure, therefore the chosen α^* for the upper part of the AH was 0.12 cm^{-1} and for the lower part was 0.04 cm^{-1}.

The results calculated from the different solutions were log transformed and plotted as box plots for each site and soil depth (Figure 4). The resulting log transformed *Kfs* values were then analysed using analysis of variance and Fisher's least significant difference (LSD) method (as described by Dytham 1999, p. 108) to determine mean significance at a 95% confidence level between the different solutions for each site and soil depth. The results of the solutions using the Fisher's LSD method are illustrated in Figure 4. Figure 4 is divided into (i) each woodland site (DW1, DW2, CW3, FW4), (ii) each grassland site (G1, G2, G3 and G4) and (iii) each floodplain site (DW1, G1 and G4). The different solutions are identified on the x-axis, as 1, 2A, 3A, 3B, 3C (and are described in Table 2). Non-shaded box plots indicate that these calculated *Kfs* values have means significantly different ($P < 0.05$) to *Kfs* values calculated by other solutions within each site. For example, in Figure 4(ii) in site G2, solution 3C has significantly lower *Kfs* values than any of the other solutions within site G2. For the Richards equation, the chosen α^* values were considered to be high (0.36 cm^{-1}) under woodland because of large macropores present in the upper soil layer. In the floodplain woodland (FW4), the upper 0.04 to 0.15 m layer intersected a more dense silt layer, therefore a lower α^* value (0.12 cm^{-1}) could be considered more appropriate. However, in the woodland areas, where *Kfs* was highly variable, mean *Kfs* values calculated from the different solutions proved not significantly different.

Under grassland and at the greater soil depth (0.15 to 0.25 m), the different solutions gave significantly different mean *Kfs* values. The upper soil layer (0.04 to 0.15 m) under grassland and the lower soil layer intersected a more permeable organic layer and then a less permeable layer, therefore the choice of α^* values was not clear. The greatest significant difference between the different solutions was the Richards equation using α^* value 0.04 cm^{-1} in comparison to 0.12 and 0.36 cm^{-1}, which corroborates the theoretical observations of Bosch (1997).

Figure 4 shows that the two Glover solutions (1 and 2A) and the Richards equation using α^* value 0.36 cm^{-1} (solution 3A) do not result in significantly different mean *Kfs* values.

Effects of smearing

Figure 5 shows the log transformed *Kfs* results as box plots to compare the different CHWP solutions against the *Kfs* results of the AH and PD methods in the floodplain

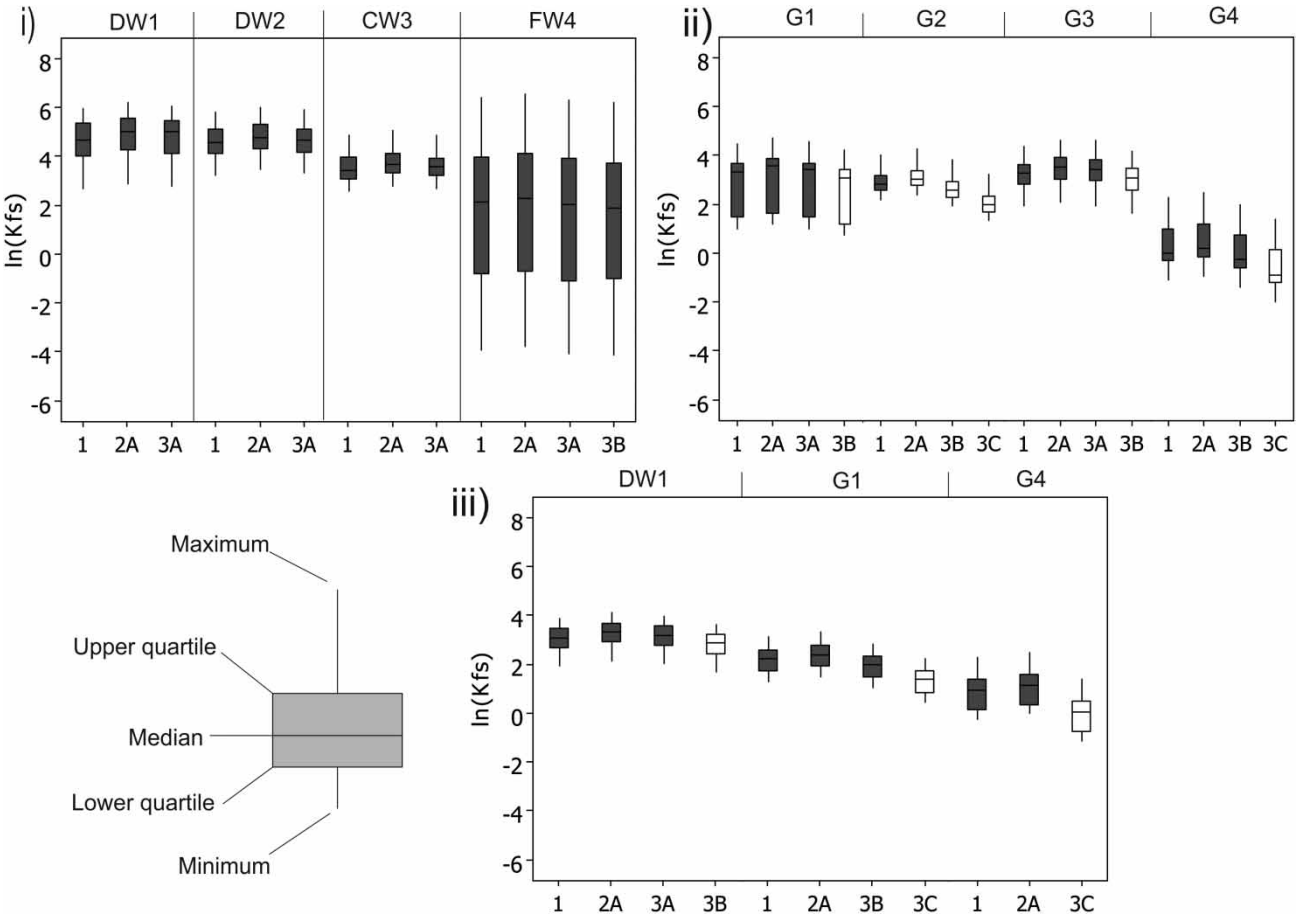

Figure 4 | Box plots illustrating *Kfs* values calculated for the different sites (located in Figure 2) using solutions 1, 2A, 3A, 3B and 3C (as described in Table 2). G1, G2, G3 and G4 are grassland areas and DW1, DW2, CW3 and FW4 are woodland areas and are explained in Table 2. Open box plots have significantly different ($P < 0.05$) mean *Kfs* values within each site group.

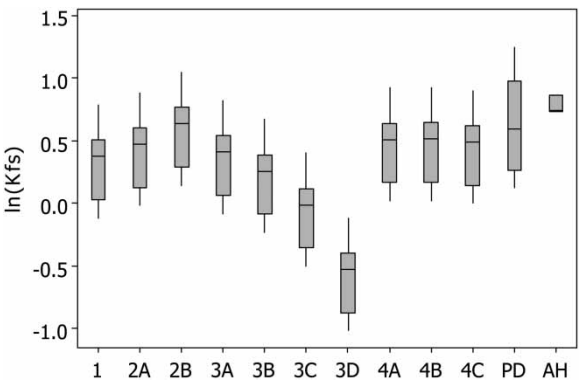

Figure 5 | Box plot comparing log transformed *Kfs* results in the floodplain area (site G4) of the CHWP solutions (1, 2A, 2B, 3A, 3B, 3C, 3D, 4A, 4B, 4C), the PD and the AH methods. The description for each solution ID is given in Table 2.

zone. Outliers were removed from the dataset, as they were considered to have been taken in gravel sediments. The three AHs measured using the AH method had *Ks* values ranging from 5.50 to 7.34 mm hour^{-1} and had a mean value of 6.13 mm hour^{-1}. The log transformed means of the CHWP solutions and the PD *Kfs* values were all found to be below the log mean AH value (Figure 5). A two-sample T-test analysis for unequal variances compared the log transformed *Kfs* values calculated by the CHWP solutions, to the AH and PD methods in the floodplain zone. All the CHWP solutions had highly significantly different *Kfs* values in comparison to the AH *Ks* values (P <0.05). Even the numerical solution (2B), which

consistently provided the highest *Kfs* values throughout the field site, had significantly lower *Kfs* values ($P = 0.033$) than the AH method *Ks* values. The PD *Kfs* values were not significantly different to solutions 2A, 2B and all the Richards equations without capillary flow (4A to 4C). The mean PD *Kfs* values were lower than the AH method values, but were not significantly different.

DISCUSSION

CHWP *Kfs* solution comparison

The lowest *Kfs* values were estimated using the Richards equation, particularly using the lowest α^* value (0.01 cm^{-1}), which decreased *Kfs* values by over 80% in comparison to the Glover solution (Table 2). The highest *Kfs* values were associated with the numerical solution derived by Reynolds *et al.* (1983) and were found to overestimate *Kfs* values by about 170% over the Glover solution, corroborating results previously noted by Reynolds *et al.* (1983). However, for the most commonly used solutions, that is, Glover solutions (1 and 2A) and Richards equations (3A and 3B), the results show that for many situations in the field site there is little significant difference in *Kfs* calculated using these different solutions (Figure 4). It is only when the soil type becomes more silty, creating a soil description which suggests a lower α^* value, that difficulties arise. Here the choice of α^* values are found to make significant differences to mean *Kfs* values (Figure 4). In the case of this study, this has particular importance because, as described in the methodology, the measured AHs intersected two different horizons, and it is difficult to select an absolute α^* value for all experimental areas. This could result in significant over or under estimation of *Kfs*, particularly if there is confusion between choosing an α^* value of 0.04 or 0.12 cm^{-1}. On the other hand, solution 2A gives consistently higher *Kfs* values and is the most comparable to the Richards equation 3A, where capillary flow has the least influence.

Choosing the 'best' solution

To choose the 'best' solution, three important site features that are relevant to *Kfs* measurements were considered.

(1) Initial soil water content: soil water contents were below field capacity, but they were moist and therefore quickly wetted-up, unlike dry soils in arid environments. AHs were also pre-wetted for at least 20 to 30 min to attain steady state (following Talsma & Hallam 1980). In combination, these two soil factors would minimise the effects of soil capillarity and therefore it is plausible to assume near-zero capillarity effects.

(2) Soil type: as outlined in the study site description, the soils measured for *Kfs* were variable not only in soil texture and structure, but also in terms of biological activity where the presence of shallow dense root mats under grassland and deep coarse roots under forest were significantly different. The glacial alluvial soils were also heterogeneous particularly within the surface profile (0.04 to 0.15 m) and at some measurement locations the AH intersected more than one horizon. This causes more than one soil textural group to occur within one AH, which makes selecting the most appropriate α^* more problematic. Thus, there exists uncertainty in the appropriate selection of α^* at some points.

(3) *H/a* ratio: Elrick *et al.* (1989) observed that *Kfs* measured using the Guelph permeameter is least sensitive to the choice of α^* when *H* is large. In cases where *H* incorporates two soil horizons and the *H* parameter is small, a question arises as to the reliability of using α^* values to estimate *Kfs* for this investigation. The particularly low *H/a* ratio also meant that gravity had a relatively large effect on *Kfs* values, as explained by Elrick & Reynolds (1992). Therefore the original Glover solution, which does not include the effect of gravity, was inappropriate to estimate *Kfs*.

Taking into account the results given in Figures 3 and 4 and Tables 2–4, the field conditions, and the low *H/a* ratios for the AHs measured, solution 2A (the Glover solution corrected for the effect of gravity) was selected as the preferred method to provide the most representative *Kfs* values for the study area. Solution 2A was thus subsequently adopted for comparison of measured *Kfs* to rainfall intensity-duration-frequency curves to infer dominant stormflow pathways (Chappell & Lancaster 2007), as undertaken by Archer *et al.* (2013).

It was also useful to examine the effect of α^* values set to infinity, to remove the effect of capillarity (solutions 4A, 4B and 4C), as this was considered to produce maximum *Kfs* values as described by Elrick *et al.* (1989). As the *Kfs* values calculated from solution 2A are lower than the resulting *Kfs* values calculated by solutions 4A, 4B and 4C, it was therefore considered that solution 2A was not overestimating *Kfs*. The numerical correction (solution 2B), on the other hand, is considered to overestimate *Kfs* values even though it was found to produce estimates of *Kfs* closer to the air entry method (Reynolds *et al.* 1983).

Effect of smearing and the over/under-estimation of CHWP *Kfs* values

The significant differences between the *Ks* values measured by the AH method and the *Kfs* values resulting from the CHWP solutions (but accepting the constraint of a small AH sample) suggest that the effect of smearing caused underestimation of *Kfs* in the floodplain zone, where the alluvial soils had a finer matrix. When comparing the AH method to the CHWP results using the Glover solution, Talsma (1987) suggested a correction factor by multiplying the CHWP results by 2 to correct for smearing on Laplace solutions. In this study, if we multiply solutions 1, 2A and 2B (variations of Laplace solutions) by 2, then solution 2B provides the closest mean *Kfs* value to the AH method, thus corroborating Talsma's (1987) conclusions.

Following on from the above findings, it is interesting to note the contrasts by other researchers in the over/underestimation of *Kfs* when comparing the other methods with solutions. According to Reynolds *et al.* (1983), the CHWP method using the Laplace solutions, that is, the Glover solution, overestimates *Kfs* when compared to the Richards equation), but according to Talsma (1987) the CHWP method using the Glover solution underestimates *Kfs* in comparison to the AH method (Talsma 1987). Even though the Richards equation provides the lowest *Kfs* of all the solutions in most studies, it is the main solution used to estimate *in situ Kfs* in the UK (Ragab & Cooper 1993; Lilly 1994; Chandler & Chappell 2008; Marshall *et al.* 2009; MacDonald *et al.* 2012). It is also worth noting that other studies have multiplied the Guelph permeameter values (calculated using the Richards equation) by 2 to obtain similar *Ks* values to the AH method (Noshadi *et al.* 2012), which they attribute to air entrapment (Bouwer 1978, p. 45).

A comparison of the surface soil *Kfs* using the PD method, to the *Kfs* as calculated by the preferred CHWP Glover solution with the effect of gravity included (solution 2A), indicates similar results. This outcome adds strength to the argument against multiplying the *Kfs* values in the floodplain zone by a factor of 2. If smearing was an issue, it would have been expected that the surface *Kfs* values (measured by the PD method) would be significantly higher than the *Kfs* values measured by the CHWP under moist soil conditions. Such remarks remain valid despite bias in the respective PD and CHWP methods towards different *Kfs* components, that is, vertical vis-à-vis horizontal.

The low *Kfs* values estimated by the Richards equation are more of a concern considering its wide use in the UK and the dependency on soil descriptions for pre-determined α^* values (Lilly 1994; Marshall *et al.* 2009; MacDonald *et al.* 2012). In this study the high silt content in the floodplain (G4) suggests an α^* value of 0.04 cm^{-1} at a depth below 0.15 m. If we used the Richards equation with this low α^* value, the resulting *Kfs* values would be significantly lower than the *Kfs* values of the AH method (as shown in Figure 5). This suggests that the effect of capillarity may not be such an issue.

In humid temperate regions where rainfall is relatively high and potential evaporation is low, moist antecedent soil conditions often close to field capacity can prevail. In such conditions, the effect of capillary flow may not be so great when measuring *Kfs* and therefore the use of the Richards equation may cause underestimation of *Kfs*. Acknowledging the persistent moist soil conditions, particularly in Scotland, saturated soil conditions enveloping AHs should easily be reached by adding water to the cavity for 20 min. Considering also the high soil structural and textural variability and the dependency of the Richards equation on an accurate estimate of α^*, the Glover solution may be more appropriate in such soil conditions.

The highest *Kfs* values recorded in this study were related to organic forest soils, which include high macro-porosity due to the presence of relatively large diameter roots, and were considered to cause some preferential flow. Germann *et al.* (2007) suggest that preferential infiltration is positioned between the domains of the Richards equation and Darcy's

law, and as suggested by Beven & Germann (2013), 'macropores carry water quite independently from antecedent soil moisture and capillary flow'. The Richards equation may therefore cause underestimations of macropore flow measured by the CHWP, so the Laplace equations may be more appropriate. However, all the equations tested ignore preferential flow, which is an important aspect particularly under forests, as experienced in this study, where organic horizons are deep and tree root systems are extensive, causing preferential flow pathways.

CONCLUSION

This comparative study illustrates the importance of understanding the antecedent soil conditions, the assumptions of existing *Kfs* equations and the environmental conditions which limit the way *Kfs* measurements are undertaken.

We found that in many situations, the results of the Glover solutions were not significantly different to the Richards equation when soil was mainly well structured or gravelly sand, providing higher α^* values (0.36 and 0.12 cm^{-1}). However, in situations where silt contents were high, the Glover solutions estimated significantly higher *Kfs* ($P < 0.05$), when α^* values were lower (≤ 0.04 cm^{-1}) in the Richards equation.

With this particular investigation in mind, we considered that solution 2A, that is, the Glover solution with gravity taken in account (Reynolds *et al.* 1983), was preferred for the following reasons:

- The Richards equation is dependent on accurate α^* values, but the measured AHs intersected soil horizon boundaries that had different soil structure and texture. Such circumstances caused difficulties within the framework of the pre-existing classification of Elrick *et al.* (1989) to select the most appropriate α^* value.
- Overestimation of solution 2A was considered to be minimal, because the resulting *Kfs* values were lower than solutions 4A, 4B and 4C (where capillarity was 0 for different soil types), which provided maximum *Kfs* values as described by Elrick *et al.* (1989).
- Within the floodplain zone where silty soils were present, *Kfs* values estimated from the CHWP method using solution 2A were significantly lower ($P > 0.05$) than estimates from the AH method, but not significantly lower than the PD method. This suggests that there were some smearing effects occurring in the floodplain zone using the CHWP method. However, as there was no order of magnitude difference in *Kfs* between these methods, unlike reports from other studies (Chappell & Lancaster 2007), the CHWP method using solution 2A was considered to give broadly representative *Kfs* values.
- Unsaturated flow could also be negligible because of the moist (not far below field capacity) soil conditions and the pre-wetting of AHs before taking measurements, following Talsma & Hallam (1980).

Taking into account various requirements for representative *Kfs* data, field conditions, constraints on measuring *Kfs* and assumptions of each solution, this study is an example of how appropriate solutions to estimate *Kfs* were chosen. The *Kfs* results secured from this study have subsequently been compared with rainfall IDF data to infer storm runoff generation processes and are described in detail in Archer *et al.* (2013).

However, none of these solutions take into account preferential flow, which could cause an underestimation of *Kfs* for all solutions. This aspect needs to be taken into account, particularly in soils that have a network of root systems, are highly organic and are biologically active, which can cause high macropore connectivity and result in preferential flow.

ACKNOWLEDGEMENTS

This research is part of the Eddleston Water Project – Phase II, which is funded by the Scottish Government. In particular we are grateful to the University of Western Australia for additional funding and equipment on which the fieldwork depended.

REFERENCES

Archer, N. A. L., Bonell, M., MacDonald, A. M., Auton, C., Coles, N. & Stevenson, R. 2013 Soil characteristics and landcover relationships on soil hydraulic conductivity at a hillslope

scale: a view towards local flood managment. *J. Hydrol.* **497**, 208–222.

Beven, K. & Germann, P. 2013 Macropores and water flow in soils revisited. *Water Resour. Res.* **49**, 3071–3092.

Boersma, L. 1965 Field measurement of hydraulic conductivity above a water table. In: *Methods of Soil Analysis* (C. A. Black, ed.). Agronomy 9, American Society of Agronomy, Madison, Wisconsin, pp. 234–252.

Bonell, M., Purandara, B. K., Venkatesh, B., Krishnaswamy, J., Acharya, H. A. K., Singh, U. V., Jayakumar, R. & Chappell, N. 2010 The impact of forest use and reforestation on soil hydraulic conductivity in the Western Ghats of India: implications for surface and sub-surface hydrology. *J. Hydrol.* **391**, 47–62.

Bosch, D. D. 1997 Constant head permeameter formula dependence on alpha parameter. *T. Am. Soc. Agri. Eng.* **40**, 1377–1379.

Bouwer, H. 1966 Rapid field measurement of air entry value and hydraulic conductivity of soil as signifiant paprameters in flow system analysis. *Water Resour. Res.* **2**, 729–723.

Bouwer, H. 1978 *Groundwater Hydrology*. McGraw-Hill, Inc, New York, USA, 480 pp.

Bouwer, H. & Jackson, R. D. 1974 Determining soil properties. In: *Drainage for Agriculture*. Vol. 17 (J. V. Schilfgaarde, ed.). American Society of Agronomy, Madison, Wisconsin, pp. 611–666.

Bown, C. J. & Shipley, B. M. 1982 *Soil Survey of Scotland: South-East Scotland, 1:250,000 Sheet 7*. The Macaulay Institute for Soil Research, University Press, Aberdeen.

British Geological Survey 2011 *Eddleston Water Catchment: Superficial Geology 1:25,000 Scale*. British Geological Survey, Keyworth, Nottingham.

Chandler, K. R. & Chappell, N. A. 2008 Influence of individual oak (Quercus robur) trees on saturated hydraulic conductivity. *Forest Ecol. Manag.* **256**, 1222–1229.

Chappell, N. A. & Lancaster, J. W. 2007 Comparison of methodological uncertainties within permeability measurements. *Hydrol. Process.* **21**, 2504–2514.

Chappell, N. A. & Ternan, J. L. 1997 Ring permeametry: design, operation and error analysis. *Earth Surf. Proc. Land.* **22**, 1197–1205.

Chappell, N. A., Sherlock, M., Bidin, K., Macdonald, R., Najman, Y. & Davis, G. 2007 Runoff processes in Southeast Asia: role of soil, regolith, and rock type. In: *Forest Environments in the Mekong River Basin* (H. Swada, M. Araki, N. A. Chappell, J. V. LaFrankie & A. Shimizu, eds). Springer-Verlag, Tokyo, pp. 2–23.

Dytham, C. 1999 *Choosing and Using Statistics*. Blackwell Science, London, 218 pp.

Elrick, D. E. & Reynolds, W. D. 1986 An analysis of the percolation test based on three-dimensional saturated-unsaturated flow from a cylindrical test hole. *Soil Sci.* **142**, 308–321.

Elrick, D. E. & Reynolds, W. D. 1992 Methods for analyzing constant-head well permeameter data. *Soil Sci. Soc. Am. J.* **56**, 320–323.

Elrick, D. E., Reynolds, W. D. & Tan, K. A. 1989 Hydraulic conductivity measurements in the unsaturated zone using improved well analyses. *Ground Water Monit. Rev.* **9**, 184–193.

Elsenbeer, H., Newton, B., Dunne, T. & de Mores, J. 1999 Soil hydraulic conductivities of latosols under pasture, forest and teak in Rondonia, Brazil. *Hydrol. Process.* **13**, 1417–1422.

Gallichand, J., Madramootoo, C., Enright, P. & Barrington, S. 1990 An evaluation of the Guelph permeameter for measuring saturated hydraulic conductivity. *Trans. ASAE* **33** (4), 1179–1184.

Germann, P., Helbling, A. & Vadilonga, T. 2007 Rivulet approach to rates of preferential infiltration. *Vadose Zone J.* **6**, 207–220.

Koppi, A. J. & Geering, H. R. 1986 The preparation of unsmeared soil surfaces and an improved apparatus for infiltration measurements. *J. Soil Sci.* **37**, 177–181.

Laase, A. D. 1989 *A Critical Evaluation of Borehole Permeameter Solutions*. New Mexico Institute of Mining and Technology. Master of Science of Hydrology, Socorro, New Mexico, p. 180.

Lilly, A. 1994 The determination of field-saturated hydraulic conductivity in some Scottish soils using the Guelph permeameter. *Soil Use Manag.* **10**, 72–78.

Lilly, A. 2000 The relationship between field-saturated hydraulic conductivity and soil structure: development of class pedotransfer functions. *Soil Use Manag.* **16**, 56–60.

MacDonald, A. M., Maurice, L., Dobbs, M. R., Reeves, H. J. & Auton, C. A. 2012 Relating in situ hydraulic conductivity, particle size and relative density of superficial deposits in a heterogeneous catchment. *J. Hydrol.* **434–435**, 130–141.

MacKenzie, D. H., 2002 Field measurement of saturated hydraulic conductivity using the well permeameter. In: *Soil Physical Measurement and Interpretation for Land Evaluation* (N. McKenzie, K. Coughlan & H. Cresswell, eds). CSIRO Publishing, Melbourne, pp. 131–149.

Marshall, M. R., Francis, O. J., Frogbrook, Z. L., Jackson, B. M., McIntyre, N., Reynolds, B., Solloway, I., Wheater, H. S. & Chell, J. 2009 The impact of upland land management on flooding: results from an improved pasture hillslope. *Hydrol. Process.* **23**, 464–475.

Mohanty, B. P., Kanwar, R. S. & Everts, C. J. 1994 Comparison of saturated hydraulic conductivty measurement methods for a glacial-till soil. *Soil Sci. Soc. Am. J.* **58**, 672–677.

Noshadi, M., Parvizi, H. & Sepaskhah, A. R. 2012 Evaluation of different methods for measuring field saturated hydraulic conductivity under high and low water table. *Vadose Zone J.* **11** (1), doi:10.2136/vzj2011.0005.

Paige, G. B. & Hillel, D. 1993 Comparison of three methods for assessing soil hydraulic properties. *Soil Sci.* **155**, 175–189.

Perroux, K. M. & White, I. 1988 Designs for disc permeameters. *Soil Sci. Soc. Am. J.* **52**, 1205–1215.

Ragab, R. & Cooper, J. D. 1993 Variability of unsaturated zone water transport parameters: implications for hydrological

modelling. 1. In situ measurements. *J. Hydrol.* **148**, 109–131.

Reynolds, W. D. & Elrick, D. E. 1986 A method for simultaneous in situ measurement in the vadose zone of field-saturated hydraulic conductivity, sorptivity and the conductivity-pressure head relationship. *Ground Water Monit. Rev.* **6**, 84–95.

Reynolds, W. D. & Elrick, D. E. 1987 A laboratory and numerical assessment of the Guelph permeameter method. *Soil Sci.* **144**, 282–299.

Reynolds, W. D., Elrick, D. E. & Topp, G. C. 1983 A reexamination of the constant head well permeameter method for measuring saturated hydraulic conductivity above the water table. *Soil Sci.* **136**, 250–268.

Salverda, A. P. & Dane, J. H. 1993 An examination of the Guelph permeameter for measuring the soil's hydraulic properties. *Geoderma* **57**, 405–421.

Scotter, D. R., Clothier, B. E. & Harper, E. R. 1982 Measuring saturated hydraulic conductivity and sorptivity using twin rings. *Aust. J. Soil Res.* **20**, 295–304.

Soil Survey of Scotland Staff 1975 *Peebles Soil Map: Soil survey of Scotland, Systematic Soil Survey; Sheet 24 & Part of Sheet 32. Scale 1:250,000*. Soil Survey of Scotland, Macaulay Institute, Aberdeen, UK.

Talsma, T. 1960 Comparison of field methods of measuring hydraulic conductivity. In International Communication on Irrigation Drainage Fourth Congress, Madrid, Spain, pp. 145–156.

Talsma, T. 1987 Re-evaluation of the well permeameter as a field method for measuring hydraulic conductivity. *Aust. J. Soil Res.* **25**, 361–368.

Talsma, T. & Hallam, P. M. 1980 Hydraulic conductivity measurement of forest catchments. *Aust. J. Soil Res.* **18**, 139–148.

Van Beers, W. F. J. 1985 *The Auger Hole Method: A Field Measurement of the Hydraulic Conductivity of Soil Below the Water Table*, 6th edn. International Institute for Land Reclamation and Improvement/ILRI, Wageningen, The Netherlands.

Wang, Z., Feyen, J., Van Genuchten, M. T. & Nielsen, D. R. 1998 Air entrapment effects on infiltration rate and flow instability. *Water Resour. Res.* **34**, 213–222.

Werritty, A., Ball, T., Spray, C., Bonell, M., Rouillard, J. & Archer, N. A. L. 2010 Restoration strategy: Eddleston Water scoping study Final Report 2010. http://www.tweedforum.org/projects/current-projects/FinalReportpdf.

World Reference Bank (WRB), IUSS Working Group 2006 World Reference Base for Soil Resoures 2006. World Soil Resources Reports No. 103. FAO, Rome.

Zangar, C. N. 1953 Theory and Problems of Water Percolation. Engineering Monograph No. 8. United States Department of the Interior, Bureau of Reclamation, Denver, Colorado, USA.

Zhang, Z. F., Groenevelt, P. H. & Parkin, G. W. 1998 The well-shape factor for the measurement of soil hydraulic properties using the Guelph Permeameter. *Soil Tillage Res.* **49**, 219–221.

First received 25 September 2012; accepted in revised form 22 January 2014. Available online 18 February 2014